Numerical Analysis of a one dimensional Diffusion Equation for a single chamber Microbial Fuel Cell using a Linked Simulation Optimization (LSO) technique

E521: Advanced Numerical Methods

Eric A. Zielke

May 5, 2006

Abstract

Renewable energy (RE) applications are becoming a popular means of power generation within our society. Microbial fuel cells (MFCs) represent a new form of renewable energy by converting organic matter into electricity by using bacteria already present in wastewater while simultaneously treating the wastewater. Increase in MFC power density by oxygen sparging can be accomplished by aerating the MFC chamber to assure sufficient reaction rates at the cathode. This study's numerical analysis includes the development and verification of FORTRAN computer code necessary to solve a one dimensional Diffusion Equation to model oxygen in a single chamber MFC. A rigorous verification of the effects of spatial and temporal discretization of the simulation model coupled to the LSO using a Modular In-Core Nonlinear Optimization System (MINOS) FORTRAN computer code was performed. Implicit Finite Difference numerical methods were found to require a substantialy larger nodal value to that of the Galerkin Finite Element approximation nodal value discretization to obtain a similar amount of error of 0.005 from the analytical solution. The cost of oxygen sparging was found to decreased substantially by a nodal discretization of 20 to 80 nodes. A realistic oxygen sparging schedules was developed by the use of 70 to 80 nodal values in a FE linear numerical method utilizing the LSO methodology.

Contents

1 Introduction **1**

2 Problem Formulation **1**

3 Literature Review **2**

3.1 MFC Technology 2

3.1.1 Biological Mechanism 2

3.1.2 Design Structure 4

3.2 Fick's Second Law 4

3.3 Implicit Finite Difference Methodology 5

3.4 Galerkin Finite Element Methodology 5

3.5 Linked Simulation Optimization Methodology 5

4 Model Formulation and Development **6**

4.1 Fick's Second Law 6

4.2 Implicit Finite Difference Methodology 7

4.3 Galerkin Finite Element Methodology 8

4.4 Optimization Model and Linked Simulation Optimization 10

4.5 Oxygen Sparging and the Diffusion Equation 12

5 Model Application **13**

5.1 System Configuration 13

5.2 Spacial and Temporal Discretizations 15

6 Model Results **15**

6.1 Numerical Variation 15

6.2 Spacial Discretization 16

6.2.1 Effect on Optimization results 20

6.3 Temporal Discretization 22

6.4 Trade-Offs 24

7 Conclusions **24**

8 Further Research **24**

9 References **26**

10 Appendix **28**

10.1 Appendix A - FD source code 28

10.2 Appendix B - FE - Linear source code 29

10.3 Appendix C - FE - Quadratic source code 30

10.4 Appendix D - FE - Cubic source code 31

10.5 Appendix E - FE - LSO - Linear source code 32

10.6 Appendix F - FE - LSO - Quadratic source code 33

10.7 Appendix G - MINOS output - Spatial Discretization 34

10.8 Appendix H - MINOS output - Temperal Discretization 35

List of Tables

1 Table of Linear, Quadratic, and Cubic Basis Functions with Associated Derivative Values (Segerlind, 1976) 10

2 Spatial and Temporal Discretization Application 15

List of Figures

1 Representation of Anaerobic (anode portion) and Aerobic (cathode portion) Biological Degradation Simultaneous to Electricity Generation in a single chamber Microbial Fuel Cell (Zielke 2006) 3

2 Representation of a single chamber Microbial Fuel Cell designed at Penn. State University (Lui and Logan 2004) 4

3 Representation of the LSO methodology to minimum oxygen sparging costs for oxygen sparging using a Galerkin FE numerical method simulation model. 12

4 Representation of a single chamber Microbial Fuel Cell modeled in one spacial dimension with oxygen concentration as the state variable and the length of the chamber equal to 310 cm. 14

5 Representation of a the FD and FE Numerical Approximations of the Diffusion Equation. The parameters selected are a diffusion value of D=20 (10E-6 mol/cm3) and 30 nodes 16

6 Close-up representation of a the FD and FE Numerical Approximations of the Diffusion Equation illustrating a large difference in the FD Numerical Approximation. The parameters selected are a diffusion value of D=20 (10E-6 mol/cm3) and 30 nodes 17

7 Close-up representation of a the FD and FE Numerical Approximations of the Diffusion Equation illustrating the difference in the FE Numerical Approximations. The parameters selected are a diffusion value of D=20 (10E-6 mol/cm3) and 30 nodes 17

8 Linear FE error residual analysis indicating a nodal value of 80 to obtain an error value of 0.005 . The parameters selected are a diffusion value of D=20 (10E-6 mol/cm3) and a time step of 0.05 seconds for a time span of 50 seconds 18

9 Quadratic FE error residual analysis indicating a nodal value of 10 to obtain an error value of 0.005. The parameters selected are a diffusion value of D=20 (10E-6 mol/cm3) and a time step of 0.05 seconds for a time span of 50 seconds. 18

10 Cubic FE error residual analysis indicating a nodal value of 25 to obtain an error value of 0.005. The parameters selected are a diffusion value of D=20 (10E-6 mol/cm3) and a time step of 0.05 seconds for a time span of 50 seconds. 19

11 Implicit FD error residual analysis indicating a nodal value of over 2000 to obtain an error value of 0.005. The parameters chosen are a diffusion value of D=20 (10E-6 mol/cm3) and a time step of 0.05 seconds for a time span of 50 seconds. 19

12 Representation of the oxygen sparging schedule for a nodal value of 20 and 80. The parameters selected are a diffusion value of D=86.4 (10E-6 mol/cm3) and 30 nodes 20

13 Representation of the cost of oxygen sparging in relation to nodal values selected in the discretization. The parameters chosen are a diffusion value of D=86.4 (10E-6 mol/cm3) and a time step of 0.05 seconds for a time span of 50 seconds. 21

14 Representation of the cost of oxygen sparging in relation to time steps selected in the discretization for a time span of 50 seconds. The parameters chosen are a diffusion value of D=86.4 (10E-6 mol/cm3) and 30 nodes 22

15 Representation of a the FE Linear Basis Function Numerical Approximation of the Diffusion Equation with a zero Neumann boundary condition approaching a steady state condition from a time span of 50 to 2000 seconds. The parameters chosen are a diffusion value of D=86.4 and 30 nodes 23

Table of Nomenclature

$$
\begin{aligned}
c &= \tfrac{mol}{cm^3} \\
L &= cm \\
[O_2] &= \tfrac{mol}{cm^3} \\
t &= s \\
D &= \tfrac{cm^2}{s} \\
x &= cm \\
Q &= \tfrac{cm^3}{s} \\
C &= [\text{US\$ } \tfrac{mol}{t}]
\end{aligned}
$$

1 Introduction

Renewable energy (RE) applications are becoming a popular means of power generation within our society. Microbial fuel cells (MFCs) represent a new form of renewable energy by converting organic matter into electricity by using bacteria already present in wastewater while simultaneously treating the wastewater. According to the Logan Group of Pennsylvania State University (PSU), this technology can use bacterium already present in wastewater as catalysts to generating electricity while simultaneously treating wastewater (Lui et al., 2004; Min and Logan, 2004). Most of the research performed on MFCs is concerned with increasing the power density of the system with respect to the peripheral anode surface area. Increase in power density by oxygen sparging can be accomplished by aerating the MFC chamber to assure sufficient reaction rates at the cathode (Lui et al., 2004). Oxygen diffusion through pure water and domestic wastewater is modeled using Fick's Second Law, or simply, the Diffusion Equation by both a Implicit Finite Difference (FD) and Galerkin Finite Element (FE) numerical analysis (Bear, 1972). The FE and FD numerical schemes of a one dimensional Diffusion Equation can utilize the Linked Simulation Optimization (LSO) methodology by generating the state variables in response to a set of oxygen concentration values (Willis and Finney, 2004).

This study's numerical analysis will include development and verification of FORTRAN computer code necessary to solve a one dimensional Diffusion Equation to model oxygen in a single chamber MFC. This study will apply a rigorous verification of the effects of spatial and temporal discretization of the simulation model coupled to the LSO using a Modular In-Core Nonlinear Optimization System (MINOS) FORTRAN computer code.

2 Problem Formulation

The objective of this study is to analyze the effects of spatial and temporal discretizations of a one dimensional Diffusion Equation by using both a FE and FD numerical analysis. The development of the FORTRAN computer codes for the Diffusion Equation will include: the Implicit FD Scheme utilizing the Thomas Algorithm, the Galerkin FE scheme with linear basis functions utilizing the Thomas Algorithm, the Galerkin FE scheme with quadratic basis functions and cubic basis functions both utilizing the Guass Siedel Algorithm. The Diffusion Equation will be used to simulate oxygen concentration values spaced from the cathode portion of the MFC to the anode portion by use of a Dirichlet initial boundary

condition and a zero Neumann final boundary condition. An optimization model used to minimize the total oxygen sparging cost (i.e. pumping cost as an oxygen source) will be developed and used in a MINOS optimization FORTRAN computer program package. The effects of total air sparging costs due to spatial and temporal discretizations will be validated by a study using the LSO methodology pertaining to a pumping policy developed for a confined groundwater aquifer (Willis and Finney, 2004).

3 Literature Review

The purpose of this literature review is to organize relevant information to use as a reference when applying principles of research and experimentation to MFC technology. This section contains an overview of MFC technology, Fick's Second Law, the Finite Difference Methodology, the Finite Element Methodology, and an overview of the LSO methodology

3.1 MFC Technology

This subsection illustrates a brief introduction to the biological and technical design characteristics pertaining to MFC technology.

3.1.1 Biological Mechanism

The basics of microbial catabolism consist of an oxidation/reduction process between a substrate and an enzyme (Bennetto 1990). This normal oxidation/reduction process consists of an electron transfer that can be harnessed in a MFC due to the characteristics of certain bacteria or microbes (Bond et al. 2002). The bacteria identified in MFCs are known as *Shewanella putrefaciens, Geobacter sulfurreducens, Geobacter metallireducens* and *Rhodoferax ferrireducens* and are commonly identified anywhere from marine sediments to domestic wastewater (Bond et al. 2003; Bond et al. 2002; Lui et al. 2004). Some research suggest that these bacteria will directly transfer an electron to any type of conductive material (Bond et al. 2003, Min 2004). In the case of a MFC, this conductive material is known as the anodic electrode and the cathodic electrode.

A simple representation of the biological mechanism is shown within a single chamber

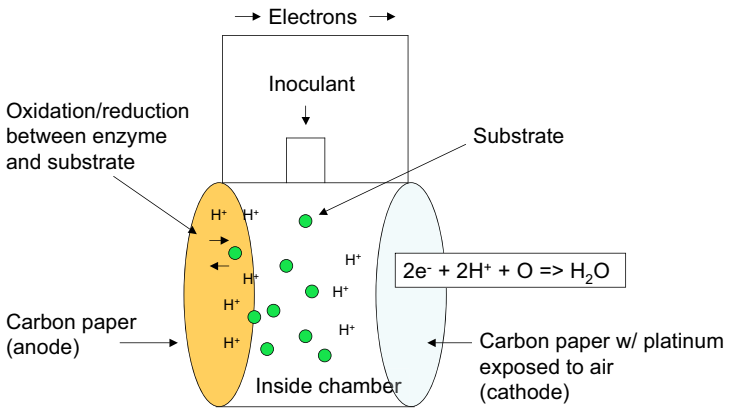

Figure 1: Representation of Anaerobic (anode portion) and Aerobic (cathode portion) Biological Degradation Simultaneous to Electricity Generation in a single chamber Microbial Fuel Cell (Zielke 2006)

MFC (Figure 1). The anode portion consists of an oxidation/reduction process which produces a hydrogen gradient and allows hydrogen protons to diffuse to the cathode portion to balance out the pH of the organic matter or wastewater originally introduced to the biological organisms in a MFC. The cathode portion also consists of this oxidation/reduction process; however, since the cathode allows oxygen to diffuse from the air to the inside portion of the single chamber MFC, water can be formed without a formation of a hydrogen proton gradient. The energy available from the proton gradient due to the anode can be harnessed by connecting a circuit from the anode to the cathode to allow the electron, oxygen and the hydrogen protons to catalytically form water via a platinum catalyst (Bond and Lovely 2003, Bond et al. 2002, Lui et al. 2004). Note that the mechanism of MFC technology is still in research stages and many possible reasons for electricity generation cannot be answered without a better understanding of the characteristics of the electricity generating bacteria in MFCs (Min 2004).

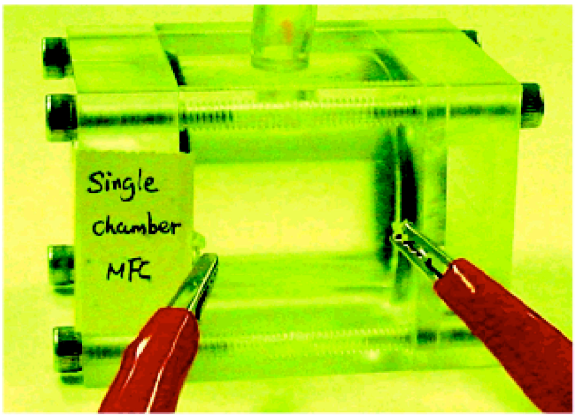

Figure 2: Representation of a single chamber Microbial Fuel Cell designed at Penn. State University (Lui and Logan 2004)

3.1.2 Design Structure

Typical MFCs consists of two separate chambers which can be inoculated with any type of carbon source liquid (i.e. biological oxygen demand (BOD) contributing liquid). These two chambers consist of an anode chamber and a cathode chamber and are generally separated by a PEM (Oh and Logan 2004). PEM fuel cell researchers know that PEMs are designed to allow oxygen from the air to react at the cathode (Lui and Logan 2004). The Logan Group suggest that this same principle can be used to design a single chamber MFC. A single chamber MFC is where the anode chamber is separated from the cathode chamber by a gas diffusion layer (GDL) or gas diffusion membrane (GDM) allowing for a passive oxygen diffusion to the cathode (Figure 2).

3.2 Fick's Second Law

Fick's Second Law, also known as the Diffusion Equation, is a case of non-steady state diffusion and is typically used in transport processes of one dimension (Plamboeck and El-Safadi, 2003). This analytical solution can be denoted as (Plamboeck and El-Safadi, 2003),

$$c = c_0 \left(erfc \frac{x}{\sqrt{2Dt}} \right)$$

Noting that the boundary values of this solution are,

$$c(0,t) = c_o$$

$$\left.\frac{dc}{dx}\right|_{x=L} = 0$$

According to Plamboeck, Ficks Second Law states, that the change of concentration in time is fast where the concentration difference across the distance is large (Plamboeck and El-Safadi, 2003).

3.3 Implicit Finite Difference Methodology

Implicit FD numerical methods are prefered over the explicit FD methods due to instability problems associated with the Explicit method (Chapra and Canale, 2002). For this reason, the Explicit method requires the Corrant condition (Chapra and Canale, 2002). The main difference between the Explicit and Implicit method is how the spatial and temporal terms are evaluated. For example, the Implict method uses an advanced time level to evaluate the spatial term (Chapra and Canale, 2002).

3.4 Galerkin Finite Element Methodology

The FE method originated from the structural analysis problems encountered in the field of civil engineering (Segerlind, 1976). The Galerkin FE method is sufficient for modeling parabolic equations such as that of the Diffusion Equation (Pinder and Gray, 1978). Although the Diffusion Equation does not include the convective term intrinsic to the convection-dispersion equation, the effect of the convective term still exists which contributes to the common oscillation, overshoot, undershoot and other undesired effects when attemping to effectively model a function of environmental systems (Pinder and Gray, 1978).

3.5 Linked Simulation Optimization Methodology

Many environmental systems are described by systems of nonlinear, coupled partial differential equations that are generally solved by FD and FE numerical methods (Willis and

Finney, 2002). These numerical methods can be used to simulate models of environmental systems; however, are generally large scaled (Willis and Finney, 2002). The linked simulation optimization methodology accomplishes optimization of large scale simulation models which would otherwise be very difficult to optimize (Willis and Finney, 2002).

4 Model Formulation and Development

This section contains Fick's Second Law, the development of the implicit FD and FE numerical approximations, the optimization model used in the MINOS optimization package coupled to the LSO methodology, and the model used for this particular study of oxygen diffusion coupled with oxygen sparging in a MFC.

4.1 Fick's Second Law

Fick's Second Law is derived from mass conservation of a species in a fluid continuum and can be expressed as (Bear, 1972),

$$\frac{\partial [O_2]}{\partial t} = D \frac{\partial^2 [O_2]}{\partial x^2}$$

where

$$\begin{aligned} [O_2] &= \text{Oxygen concentration} \\ t &= \text{time} \\ D &= \text{Diffusion coefficient} \\ x &= \text{length} \end{aligned}$$

with boundary conditions,

$$[O_2](0,t) = [O_2]_o$$

$$\left. \frac{d[O_2]}{dx} \right|_{x=L} = 0$$

4.2 Implicit Finite Difference Methodology

The Implicit FD methodology evaluates first order derivative terms by use of a backward finite-divided difference formula derived from the Taylor series expansion (Chapra and Canale, 2002). This formula can be expressed as,

$$\left.\frac{df}{dx}\right|_x = \frac{f(x) - f(x - \triangle x)}{\triangle x}$$

The backward difference formula contains a truncation error order of one. Second order derivative terms are evaluated by use of a centered finite-divided difference formula derived from the Taylor series expansion containing a truncation error order of two, i.e. less error then that of the backward difference (Chapra and Canale, 2002). This formula is generally expressed as,

$$\left.\frac{d^2f}{dx^2}\right|_x = \frac{f(x + \triangle x) - 2f(x) + f(x - \triangle x)}{\triangle x^2}$$

After a discretization nodal scheme has been established, a general finite difference equation can be expressed as,

$$D\left\{\frac{[O_2]_{i+1} - 2[O_2]_i + [O_2]_{i-1}}{\triangle x^2}\right\} = \frac{[O_2]_i}{dt}$$

This general equation can then written for every node. Noting that the boundary conditions will be placed in the f bar, vector notation for a three internal nodal system can be expressed as,

$$\begin{bmatrix} -\frac{2D}{\triangle x^2} & \frac{D}{\triangle x^2} & 0 & 0 \\ \frac{D}{\triangle x^2} & -\frac{2D}{\triangle x^2} & \frac{D}{\triangle x^2} & 0 \\ 0 & \frac{D}{\triangle x^2} & -\frac{2D}{\triangle x^2} & \frac{D}{\triangle x^2} \\ 0 & 0 & \frac{D}{\triangle x^2} & -\frac{2D}{\triangle x^2} \end{bmatrix} \begin{bmatrix} [O_2]_1 \\ [O_2]_2 \\ [O_2]_3 \\ [O_2]_4 \end{bmatrix} + \begin{bmatrix} \frac{D}{\triangle x^2}[O_2]_0(t) \\ 0 \\ 0 \\ \frac{D}{\triangle x^2}[O_2]_5(t) \end{bmatrix} = \begin{bmatrix} [\dot{O}_2]_1 \\ [\dot{O}_2]_2 \\ [\dot{O}_2]_3 \\ [\dot{O}_2]_4 \end{bmatrix}$$

Now the equation can be solved for implicitly as follows,

$$A\frac{\underline{[O_2]}^t - \underline{[O_2]}^{t-\triangle t}}{dt} + B\underline{[O_2]}^t + \underline{f}^t = \underline{0}$$

rearranging to the form A$\underline{x}$=$\underline{b}$,

$$\left\{\frac{A}{\triangle t} + B\right\}\underline{[O_2]}^t = \frac{A}{\triangle t}\underline{[O_2]}^{t-1} - \underline{f}^t$$

Since the coefficient matrix is tridiagonal and sparse, the solution of these linear Odinary Differential Equations (ODEs) can be solved using a Thomas Algorithm. A formulation of

the FORTRAN computer source code can be found in Appendix A.

4.3 Galerkin Finite Element Methodology

One FE formulation scheme is known as the method of weighted residuals where the desired function $[O_2]$ is replaced by a finite series approximation $[\hat{O}_2]$ which is generally expressed as (Lapidus and Pinder, 1982),

$$[O_2] \approx [\hat{O}_2] = \sum_{i=1}^{n} N_i(x)\widetilde{[O_2]}_i(t)$$

where

$$\begin{aligned} N_i &= \text{Interpolating functions} \\ \widetilde{[O_2]}_i &= \text{Undetermined coefficients} \end{aligned}$$

The Galerkin method is a special case of the the method of weighted residuals when the weighting function is chosen to be the basis function and expressed as (Lapidus and Pinder, 1982),

$$\int\int\int_{N_i} L\{[\hat{O}_2]\} = 0, \quad \forall_i$$

The above function implies that there exists N equations requiring N basis functions that need to be solved for simultaneously. The finite elementization of Fick's Second Law can be expressed as,

$$\int_0^L N_i \left\{ D\frac{\partial^2 \underline{N}[O_2]}{\partial x^2} - \frac{(\underline{N}[O_2])}{\partial t} \right\} dx = 0, \quad \forall_i$$

Note that the next objective requires reducing the above equation into a form of,

$$A\underline{[\dot{O}_2]} + B\underline{[O_2]} + \underline{f} = \underline{0}$$

By using integration by parts, the Diffusion term can be evaluated in the B elemental matrix. For linear basis functions, the 2×2 elemental matrix expression is,

$$-D \begin{bmatrix} \int_{L_e} \frac{\partial N_i}{\partial x}\frac{\partial N_i}{\partial x}dx & \int_{L_e} \frac{\partial N_i}{\partial x}\frac{\partial N_j}{\partial x}dx \\ \int_{L_e} \frac{\partial N_j}{\partial x}\frac{\partial N_i}{\partial x}dx & \int_{L_e} \frac{\partial N_j}{\partial x}\frac{\partial N_j}{\partial x}dx \end{bmatrix} \begin{bmatrix} [O_2]_i \\ [O_2]_j \end{bmatrix}$$

The temporal term can be evaluated in the A elemental matrix for linear basis function as,

$$\begin{bmatrix} \int_{L_e} N_i N_i dx & \int_{L_e} N_i N_j dx \\ \int_{L_e} N_j N_i dx & \int_{L_e} N_j N_j dx \end{bmatrix} \begin{bmatrix} [\dot{O}_2]_i \\ [\dot{O}_2]_j \end{bmatrix}$$

The Dirichlet initial boundary condition and zero-Neumann boundary condition placed at the end of the model length are eveluated in the f bar vector for the global system of equations. This can be expressed as,

$$\begin{bmatrix} -D\frac{\partial [O_2]}{\partial x}\Big|_{z=0} \\ \cdot \\ \cdot \\ \\ -D\frac{\partial [O_2]}{\partial x}\Big|_{z=L} \end{bmatrix}$$

For a simple four nodal or three elemental system assuming a Dirichlet initial boundary condition and zero-Nuemann boundary condition placed at the maximum length of the system, the formation of converting the elemental matrixes to the global matrix can be expressed as,

$$\begin{bmatrix} I_a\ II_a & II_a & \\ II_a & II_a\ III_a & III_a \\ & III_a & III_a \end{bmatrix} \begin{bmatrix} [\dot{O}_2]_2 \\ [\dot{O}_2]_3 \\ [\dot{O}_2]_4 \end{bmatrix} + \begin{bmatrix} I_b\ II_b & II_b & \\ II_b & II_b\ III_b & III_b \\ & III_b & III_b \end{bmatrix} \begin{bmatrix} [O_2]_2 \\ [O_2]_3 \\ [O_2]_4 \end{bmatrix} + \begin{bmatrix} [O_2]_0 \times I_b(2,1) \\ 0 \\ 0 \end{bmatrix} = \underline{0}$$

Note that quadratic basis functions will yield a 3×3 elemental matrix and cubic basis functions will yield a 4×4 elemental matix. The values of these basis functions are commonly expressed in literature in which each associated derivative value can be computed with a graphing calculator (Table 1).

Table 1: Table of Linear, Quadratic, and Cubic Basis Functions with Associated Derivative Values (Segerlind, 1976)

	Basis Function	Derivative of Basis Function
Linear	$N_i = 1 - \frac{x}{L_e}$	$\frac{dN_i}{dx} = -\frac{1}{L_e}$
	$N_j = \frac{x}{L_e}$	$\frac{dN_j}{dx} = \frac{1}{L_e}$
Quadratic	$N_i = \left(1 - \frac{2x}{L_e}\right)\left(1 - \frac{x}{L_e}\right)$	$\frac{dN_i}{dx} = \frac{4x}{(L_e)^2} - \frac{3}{L_e}$
	$N_j = \frac{4x}{L_e}\left(1 - \frac{x}{L_e}\right)$	$\frac{dN_j}{dx} = \frac{4}{L_e} - \frac{8x}{(L_e)^2}$
	$N_k = -\frac{x}{L_e}\left(1 - \frac{2x}{L_e}\right)$	$\frac{dN_k}{dx} = \frac{4x}{(L_e)^2} - \frac{1}{L_e}$
Cubic	$N_i = \left(1 - \frac{3x}{L_e}\right)\left(1 - \frac{3x}{2L_e}\right)\left(1 - \frac{x}{L_e}\right)$	$\frac{dN_i}{dx} = -\frac{11}{2L_e} + \frac{18x}{(L_e)^2} - \frac{27x^2}{2(L_e)^2}$
	$N_j = \frac{9x}{L_e}\left(1 - \frac{3x}{2L_e}\right)\left(1 - \frac{x}{L_e}\right)$	$\frac{dN_j}{dx} = \frac{9}{L_e} - \frac{45x}{(L_e)^2} + \frac{81x^2}{2(L_e)^3}$
	$N_k = -\frac{9x}{2L_e}\left(1 - \frac{3x}{L_e}\right)\left(1 - \frac{x}{L_e}\right)$	$\frac{dN_k}{dx} = -\frac{9}{2L_e} + \frac{36x}{(L_e)^2} - \frac{81x^2}{2(L_e)^3}$
	$N_l = \frac{x}{L_e}\left(1 - \frac{3x}{L_e}\right)\left(1 - \frac{3x}{2L_e}\right)$	$\frac{dN_l}{dx} = \frac{1}{L_e} - \frac{9x}{(L_e)^2} + \frac{27x^2}{2(L_e)^3}$

Using the values for the basis functions, values for the integrals of the linear, quadratic, and cubic elemental matrixes can be seen in the FORTRAN source code (Appendix B; C; and D).

4.4 Optimization Model and Linked Simulation Optimization

The optimization model used in this study minimizes the total costs for oxygen sparging in a MFC. The model is simply a modification of total cost minimization of groundwater extraction (Willis and Finney, 2002),

$$\min z = \sum_{i=1}^{n} 10Q_i(50 - [O_2]_i)$$

the oxygen demand constraint is,

$$\sum_{i=1}^{n} Q_i = 350$$

and the non-negativity associated with the control variables,

$$Q_i \geq 0, \quad \forall_i$$

This model assumes oxygen sparging (i.e. pumping) cost for placement i to equal (Willis and Finney, 2002),

$$C_i = 10Q_i(50 - [O_2]_i)$$

where

$$\begin{aligned} C_i &= \text{the cost [US\$ } \tfrac{mol}{t}] \\ 10 &= \text{ cost of oxygen sparging/pumping [US\$]} \\ Q_i &= \text{oxygen sparging/pumping at site}i \ [\tfrac{L^3}{t}] \\ 50 &= \text{maximum amount of oxygen concentration } [\tfrac{mol}{L^3}] \\ [\mathrm{O_2}] &= \text{oxygen concentration at site } i \ [\tfrac{mol}{L^3}] \end{aligned}$$

The optimization model is transfered to a FORTRAN computer code subroutine called $funobj$ to be used by the simulation FORTRAN subroutine using the Galerkin FE simulation model. The process of this study's LSO problem begins with MINOS sending the decision variable of the oxygen sparging/pumping rate to $funobj$. $Funobj$ then supplies the decision variables to the Galerkin FE simulation model. The simulation model generates the state variable of oxygen concentration to $funobj$ to evaluate the objective value. The objective value is then passed to MINOS to start the process over again until an optimal solution is found. A schematic of the LSO for this program is shown in Figure 3. A formulation of the subroutines using a Galerkin FE simulation model with linear basis functions and a Galerkin FE simulation model using quadratic basis functions can be seen in Appendix E and Appendix F.

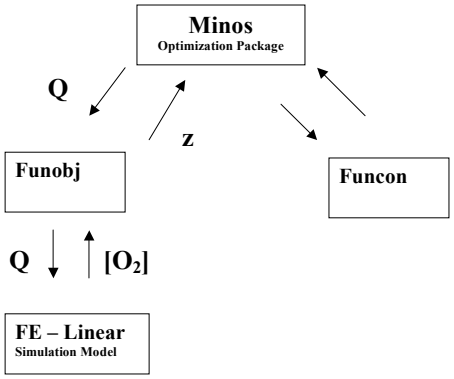

Figure 3: Representation of the LSO methodology to minimum oxygen sparging costs for oxygen sparging using a Galerkin FE numerical method simulation model.

4.5 Oxygen Sparging and the Diffusion Equation

Considering a non-steady state diffusion such as dictated by Fick's Second Law, a mathematical model of the MFC system can be expressed as,

$$D\frac{\partial^2[O_2]}{\partial x^2} - \frac{\partial[O_2]}{\partial t} + \sum_i Q_i\delta(x - x_i) = 0$$

where

$$\begin{aligned} [O_2] &= \text{Oxygen concentration} \\ t &= \text{time} \\ D &= \text{Diffusion coefficient} \\ x &= \text{length} \\ Q_i &= \text{oxygen sparging rate} \\ \delta &= \text{Dirac delta function} \end{aligned}$$

with boundary conditions,

$$[O_2](0,t) = [O_2]_o$$

$$\left.\frac{d[O_2]}{dx}\right|_{x=L} = 0$$

The Dirac delta function is used to define the location of the oxygen sparging throughout the MFC system. Oxygen sparging in this model is replicated upon hydraulic pumping as a source in contrast to more common hydraulic pumping schemes modeled as a sink (Willis and Finney, 2002).

5 Model Application

This section details the application of Fick's Second Law to a system configuration with relevant parameters. This section will also detail the process of both spacial and temporal discretization techniques performed on the FD and FE numerical methods and the LSO.

5.1 System Configuration

This study will analyze the diffusion of oxygen in relation to time and one-dimensional space through a MFC. A simple representation of the configuration is given in Figure 4. A time-span of 50 seconds is a desirable length of time to investigate due to the microbial activity that would begin to take place after any amount of time after 50 seconds. After 50 seconds, the oxidation/reduction process is assumed to take place between oxygen and the microbes present in the MFC and thus, affect the diffusion of oxygen in a way that this particular model would not be able to represent. Studies have reported values of 18.7×10^{-6} $\frac{cm^2}{s}$ to 26×10^{-6} $\frac{cm^2}{s}$ as values for oxygen diffusion through pure water (Yapar et. al., 2000). This study selected a value of 20×10^{-6} for oxygen diffusion. For the data acquired by the

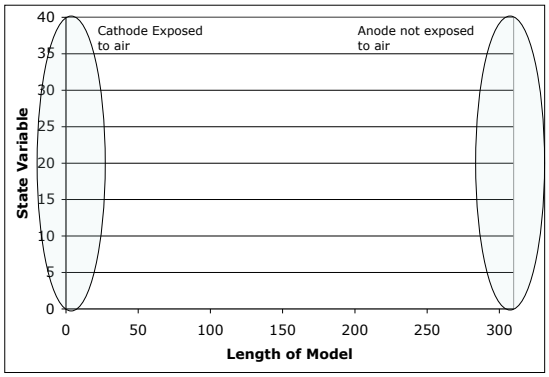

Figure 4: Representation of a single chamber Microbial Fuel Cell modeled in one spacial dimension with oxygen concentration as the state variable and the length of the chamber equal to 310 cm.

LSO output, a value of 86.4×10^{-6} $\frac{cm^2}{s}$ was used as an oxygen diffusion value pertaining to the maximum possible value of oxygen diffusion through water (Yapar et. al., 2000). The system assumes 40×10^{-3} $\frac{mol}{cm^3}$ oxygen concentration as the initial Dirichlet boundary condition and a zero Neumann condition placed at the anode 310 cm at length from the cathode. The rational for a zero Neumann condition placed at the anode is based upon the construction and physical characteristics of a MFC. As illustrated in Figure 1, there is no possibility of oxygen diffusion through the anode since the anode is not exposed to air in contrast to the cathode which is exposed to air. However, there is no knowledge of the actual concentration of oxygen present at the anode location in which this study used to justify why a zero Neumann boundary condition is a more accurate then a zero Dirichlet boundary condition. Note there is no data available to quantify how accurate these boundary conditions are in relation to what would take place in a MFC; however, this study is not concerned with how accurate this model relates to what would take place in a MFC, but rather the effects of spacial and temporal discretizations in the numerical methods used to model oxygen diffusion and oxygen sparging and how these discretizations effect the output of the model.

5.2 Spacial and Temporal Discretizations

Spacial discretizations were performed for each FD and FE numerical method program developed except for the the FE program utilizing quadratic basis functions implemented in the LSO due to undesired 30-60 minute run-times required for each discretization. Temporal discretizations were not investigated for every program due to lack of noticable variation of the state variable with respect to the given time step and a time span of 50 seconds. Every program was ran to a steady steady state solution by increasing the time span to a large magnitude of 2000 seconds or roughly one half hour.

Table 2: Spatial and Temporal Discretization Application

	Implicit FD	FE - Linear	FE - Quadratic	FE - Cubic
Spacial (nodes)	10 - 2000+	20 - 200	8 - 30	3 - 50
Spacial in LSO (nodes)	no code	10 - 80	30	no code
Temporal (time step)	N/A*	0.05 - 50	N/A*	N/A*
Temporal in LSO (time step)	no code	0.05 - 50	N/A*	no code

*code is available

6 Model Results

This section provides a thorough illustration and discussion of the model results corresponding to the application. More emphasis is given to spacial discretization than that of temporal discretization.

6.1 Numerical Variation

There exists numerical variations of oxygen concentration values throughout all four numerical schemes developed for this study (Figure 5). A closer look at the difference between the numerical approximations indicate a large difference between the FD numerical approximation to that of the FE numerical approximation (Figure 6). Further visual investigation indicate an actual piece-wise approximation difference between the FE schemes utilizing linear, quadratic and cubic basis function (Figure 7).

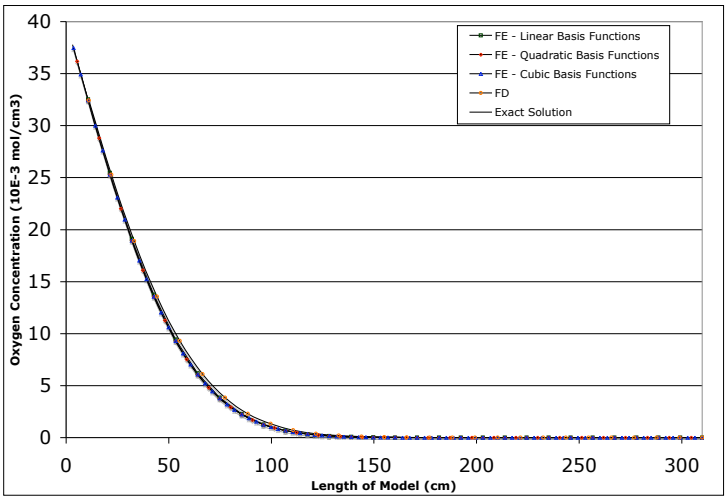

Figure 5: Representation of a the FD and FE Numerical Approximations of the Diffusion Equation. The parameters selected are a diffusion value of D=20 (10E-6 mol/cm3) and 30 nodes

6.2 Spacial Discretization

The results of spacial discretization indicate large variations of oxygen concentration in relation to the number of nodes or elements selected in the discretization. Values of the sumation of squared residuals for each of the four computer programs indicated that the Implicit FD numerical approximation is highly dependent on large nodal values to fall within an error value of 0.005 in comparison to the values of oxygen concentration obtained from the Galerkin FE numerical approximations (Figure 8; 9; 10; 11).

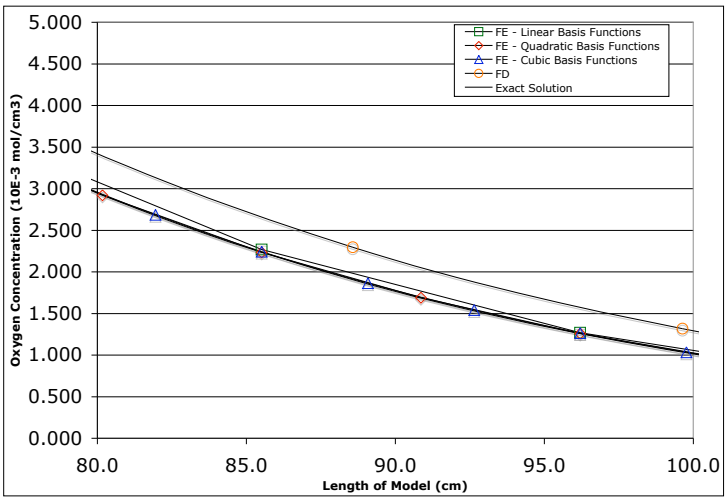

Figure 6: Close-up representation of a the FD and FE Numerical Approximations of the Diffusion Equation illustrating a large difference in the FD Numerical Approximation. The parameters selected are a diffusion value of D=20 (10E-6 mol/cm3) and 30 nodes

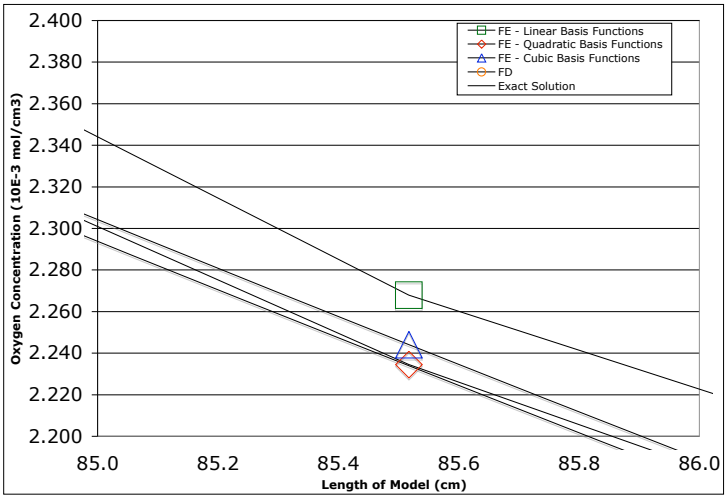

Figure 7: Close-up representation of a the FD and FE Numerical Approximations of the Diffusion Equation illustrating the difference in the FE Numerical Approximations. The parameters selected are a diffusion value of D=20 (10E-6 mol/cm3) and 30 nodes

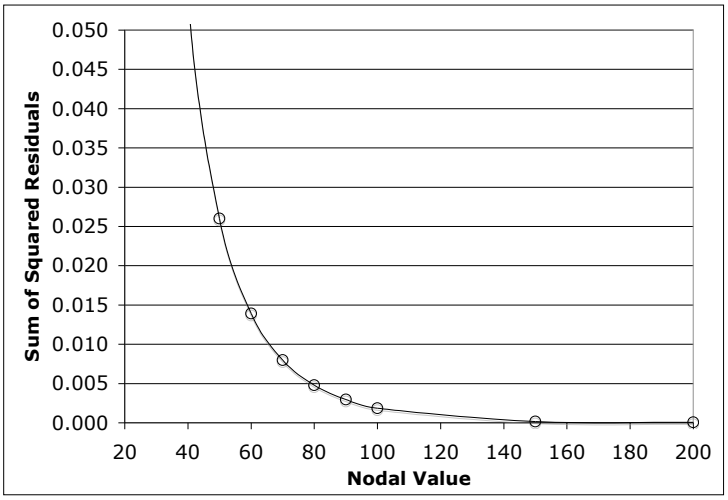

Figure 8: Linear FE error residual analysis indicating a nodal value of 80 to obtain an error value of 0.005 . The parameters selected are a diffusion value of D=20 (10E-6 mol/cm3) and a time step of 0.05 seconds for a time span of 50 seconds

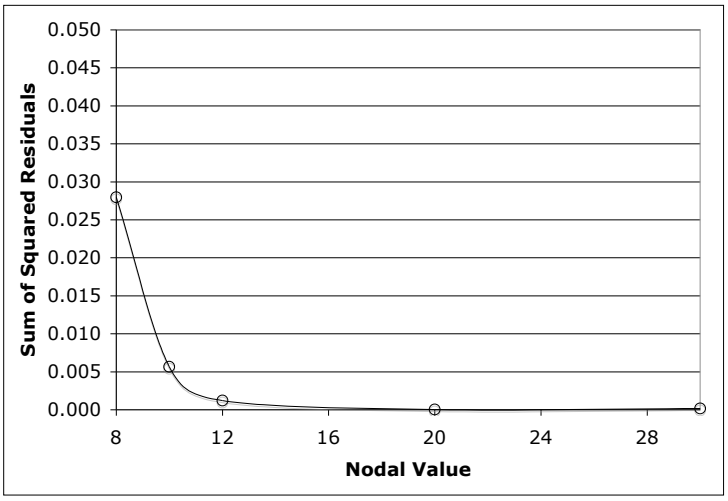

Figure 9: Quadratic FE error residual analysis indicating a nodal value of 10 to obtain an error value of 0.005. The parameters selected are a diffusion value of D=20 (10E-6 mol/cm3) and a time step of 0.05 seconds for a time span of 50 seconds.

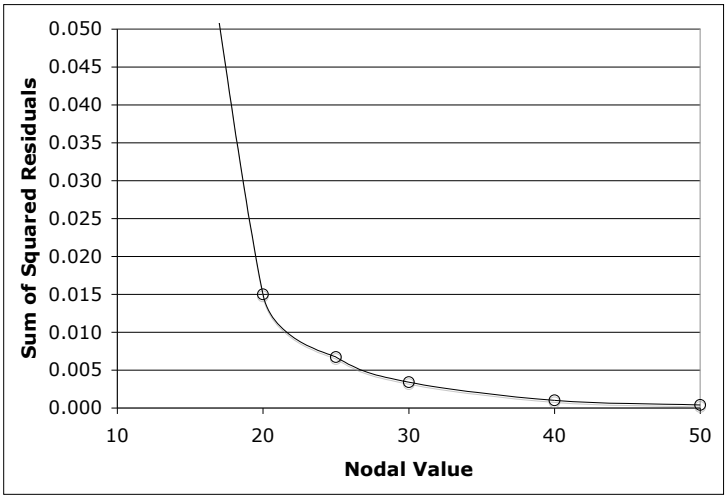

Figure 10: Cubic FE error residual analysis indicating a nodal value of 25 to obtain an error value of 0.005. The parameters selected are a diffusion value of D=20 (10E-6 mol/cm3) and a time step of 0.05 seconds for a time span of 50 seconds.

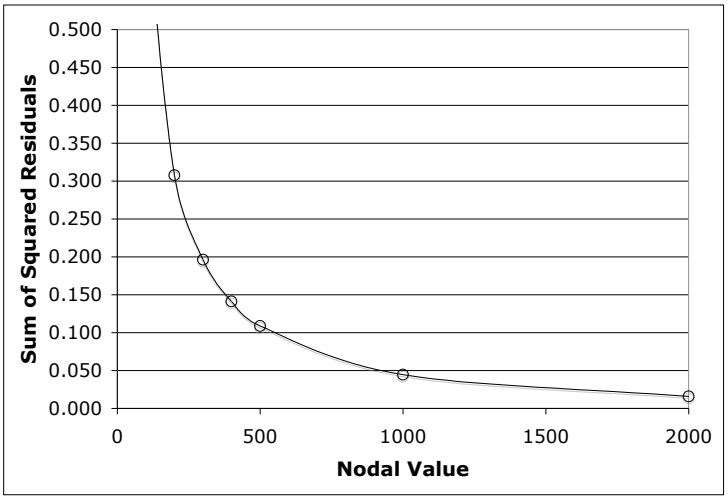

Figure 11: Implicit FD error residual analysis indicating a nodal value of over 2000 to obtain an error value of 0.005. The parameters chosen are a diffusion value of D=20 (10E-6 mol/cm3) and a time step of 0.05 seconds for a time span of 50 seconds.

6.2.1 Effect on Optimization results

Spacial discretization effects the oxygen sparging values (Figure 12). At a nodal value of 20, the optimization scheme suggests pumping values that would indicate negative oxygen concentrations which is not physically possible. Only until a nodal value of 70 or 80 is selected are more realistic results obtained (Figure 12; Appendix 6).

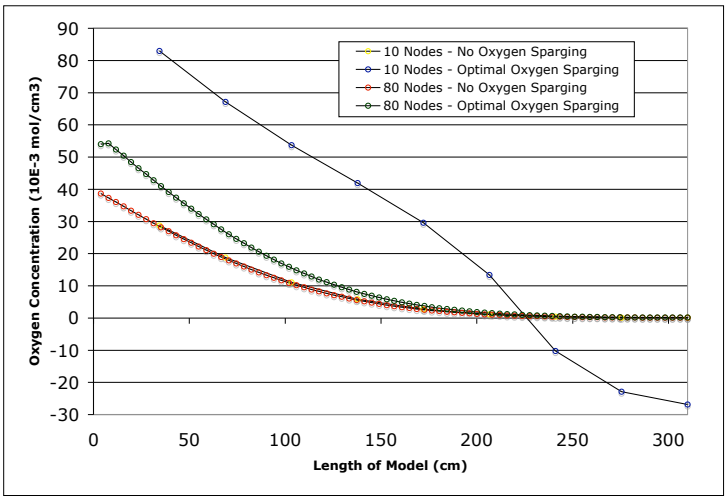

Figure 12: Representation of the oxygen sparging schedule for a nodal value of 20 and 80. The parameters selected are a diffusion value of D=86.4 (10E-6 mol/cm3) and 30 nodes

The effect of spacial discretization affects the optimal cost of oxygen sparging (Figure 13). This graph shows a substantial decrease in cost due to nodal discretization.

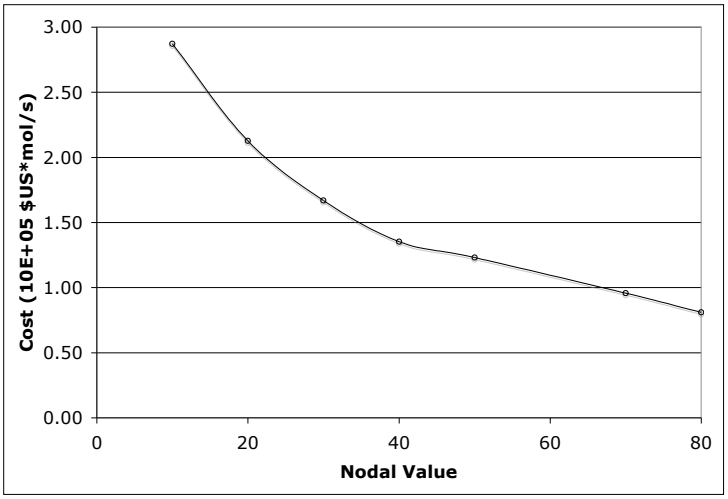

Figure 13: Representation of the cost of oxygen sparging in relation to nodal values selected in the discretization. The parameters chosen are a diffusion value of D=86.4 (10E-6 mol/cm3) and a time step of 0.05 seconds for a time span of 50 seconds.

6.3 Temporal Discretization

This particular study did not investigate temporal discretization to the extent of spacial discretization due to a lack of noticable significance in the variation of oxygen concentration values with respect to the discretization. However, an investigation of the optimal cost was recorded with respect to the temporal discretization (Figure 14). The values of cost are not nearly as significant to that of spacial discretization.

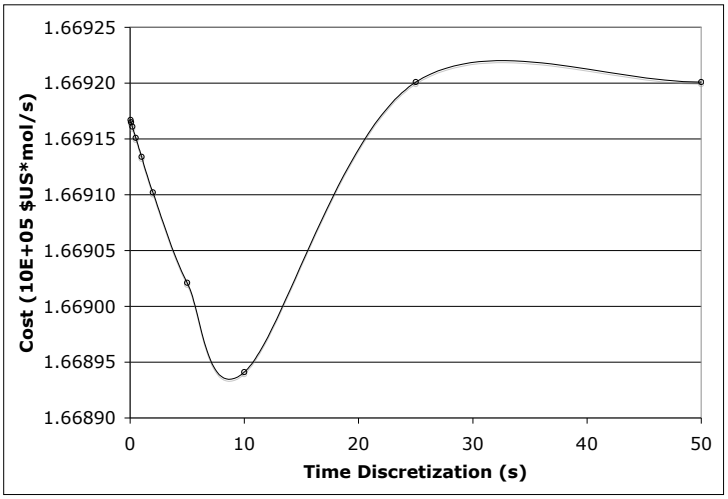

Figure 14: Representation of the cost of oxygen sparging in relation to time steps selected in the discretization for a time span of 50 seconds. The parameters chosen are a diffusion value of D=86.4 (10E-6 mol/cm3) and 30 nodes

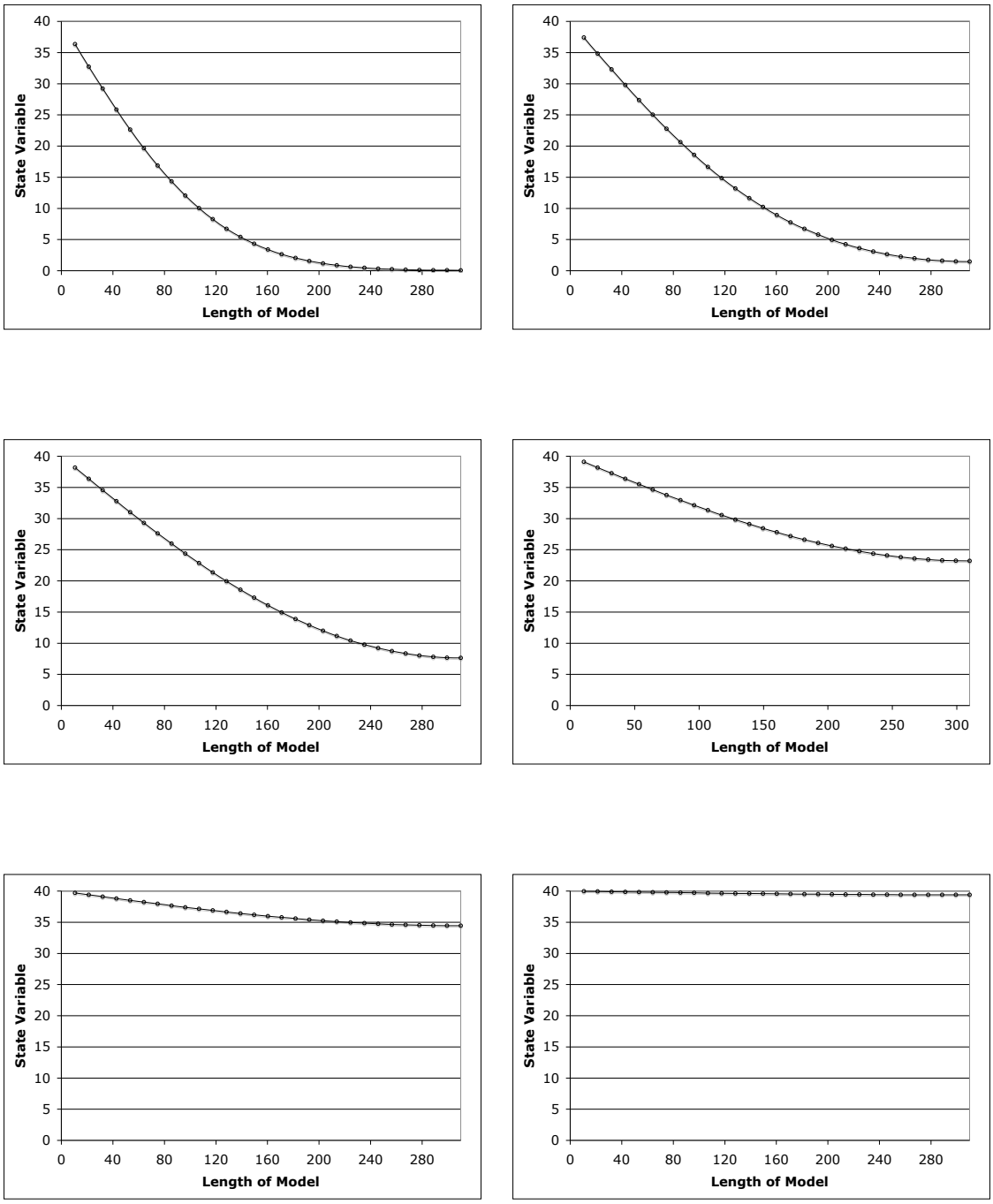

Figure 15: Representation of a the FE Linear Basis Function Numerical Approximation of the Diffusion Equation with a zero Neumann boundary condition approaching a steady state condition from a time span of 50 to 2000 seconds. The parameters chosen are a diffusion value of D=86.4 and 30 nodes

6.4 Trade-Offs

The most common trade-off associated with numerical methods involve selecting either a FD or FE approach in environmental systems (Chapra and Canale, 2002). FD approximations are perhaps more intuitive and thus easier to program; however, when an environmental system involves non-uniform and heterogenoues conditions, FE approximations are superior to that of FD (Chapra and Canale, 2002). The trade-off is the computation time and effort required by that of the FE numerical method.

7 Conclusions

The results of this study indicate that the type of numerical method chosen and discretization selected will dictate the value of the state variable associated with a model used in environmental systems. Specifically, the investigation shows the following:

• Implicit Finite Difference numerical methods require a substantialy larger nodal value to that of the Galerkin Finite Element approximation nodal value discretization to obtain a similar amount of error from the analytical solution.
• Temporal discretizations have little effect to the approximation values and optimization values in comparison to the spatial discretizations.
• The trade-off of a FD numerical scheme to that of a FE scheme is accuracy to computational time and effort.
• The cost of oxygen sparging is decreased substantially by a proper nodal discretization of 20 to 80 nodes
• Realistic oxygen sparging schedules can be developed by the use of 70 to 80 nodal values in a FE linear numerical method utilizing the LSO methodology.

8 Further Research

This study was preliminary in development for a optimization scheme to be used in a linked simulation optimization methodology in conjunction with a partial differential equation. Further investigation would be desireable to develop an optimization scheme that would

take into quantitative account the potential benefits obtained from oxygen sparging in a MFC.

9 References

Bhattacharjya, R; Datta, B; Optimal Management of Coastal Aquifers Using Linked Simulation Optimization Approach. *Water Resources Management.* **2005**, 19, 295320

Bear, J; *Dynamics of Fluids in Porous Media.* American Elsevier. New York. **1972**

Chapra, S; Canale, R; *Numerical Methods for Engineers.* McGraw-Hill. New York. **2002**
Lapidus, L; Pinder, G; *Numerical Solution of Partial Differential Equations in Science and Engineering* John Wiley and Sons. New York. **1982**

Lui, H.; Cheng, S; Logan, B.E.; Production of Electricity from Acetate or Butyrate Using a Single Chamber Microbial Fuel Cell. *Environ. Sci. Tech.* **2005**, 39, 658-662

Lui, H.; Logan, B.E.; Electricity generation using an air-cathode single chamber microbial fuel cell in the presence and absence of a proton exchange membrane. *Environ. Sci. Tech.* **2004**, 38, 4040-4046

Lui, H,; Ramnarayanan, R.; Logan, B.E.; Production of electricity during wastewater treatment using a single chamber microbial fuel cell. *Environ. Sci. Tech.* **2004**, 38, 2281-2285

Min, B.; Logan, B.E.; Continuous electricity generation from domestic wastewater and organic substrates in a flat plate microbial fuel cell. *Environ. Sci. Tech.* **2004**, 38, 5809-5814

Oh, S.; Min, B.; Logan, B.E.; Cathode performance as a factor in electricity generation in Microbial Fuel Cells. *Environ. Sci. Technol.* **2004**, 38, 4900-4904

Pinder, G; Gray, W; *Finite Elements in Water Resources.* Pentech Press. London. **1978**.

Plamboeck, C; El-Safadi, H; Mass transfer across two-fluid interfaces in microfluid systems. *Mikroelektronik Centret* **2003**

Segerlind, L; *Applied Finite Element Analysis.* John Wiley and Sons. New York. **1976**

Singh, R; Datta, B; Identification of Groundwater Pollution Sources Using GA-based Linked Simulation Optimization Model. *Journal of Hydrologic Engineering* **2006**, 109, March/April

Yapar, S; Peker, S; Kuryel, B; Difusion of Oxygen to Aqueous Surfactant Solutions. *Turk J Engin Environ Sci* **2000**, 24, 365-372.

Willis, R; Finney, B; *Environmental Systems Engineering and Economics.* Kluwer Academic Publishers. Boston. **2004**

Willis, R.; Finney, B; Personal Communication. January - April, 2006.

Zielke, E.A.; Design of a Single Chamber Microbial Fuel Cell. *Pennsylvania State University webpage.* http://www.engr.psu.edu/ce/enve/mfc-Logan_files/mfc-makeone.htm **2006.**

10 Appendix

10.1 Appendix A - FD source code

10.2 Appendix B - FE - Linear source code

10.3 Appendix C - FE - Quadratic source code

10.4 Appendix D - FE - Cubic source code

10.5 Appendix E - FE - LSO - Linear source code

10.6 Appendix F - FE - LSO - Quadratic source code

10.7 Appendix G - MINOS output - Spatial Discretization

10.8 Appendix H - MINOS output - Temperal Discretization